Haptic identification by ELM-controlled uncertain manipulator

Article (Accepted Version)

Haptic Identification by ELM Controlled Uncertain Manipulator

Chenguang Yang, *Senior Member, IEEE*, Kunxia Huang, Hong Cheng, *Senior Member, IEEE*, Yanan Li, *Member, IEEE*, and Chun-Yi Su, *Senior Member, IEEE*

***Abstract*—This paper presents an extreme learning machine (ELM) based control scheme for uncertain robot manipulators to perform haptic identification. ELM is used to compensate for the unknown nonlinearity in the manipulator dynamics. The ELM enhanced controller ensures that the closed-loop controlled manipulator follows a specified reference model, in which the reference point as well as the feedforward force is adjusted after each trial for haptic identification of geometry and stiffness of an unknown object. A neural learning law is designed to ensure finite-time convergence of the neural weight learning, such that exact matching with the reference model can be achieved after the initial iteration. The usefulness of the proposed method is tested and demonstrated by extensive simulation studies.**

***Index Terms*—Extreme learning machine; haptic identification; adaptive control; robot manipulator.**

I. Introduction

The evolution of robot technologies starts from industrial applications such as simple functions of casting, forging, stamping and welding etc [1]. With the advance of sensing technologies, it brings more perceptive functions to robots to excute a variety of complicated tasks, e.g., autonomous navigation of mobile robots with the ability of sensing the surrounding environment to plan a path and to perform relevant tasks [2]. In addition to industrial applications, robots have also been widely applied in service and medical fields. In these fields, a robot is supposed to interact with a dynamic environment and to manipulate unknown objects. Thus, it is necessary for a robot to learn and recognize the properties of the environment and objects, such as elasticity, geometry and so on. For this purpose, visual sensing technique has become mature and widely used technique [3], e.g., a stereo camera was applied to acquire the position of target objects for a grasping task in a hand-eye robot system [4]. However, when the lighting condition in the working environment is bad, e.g., either too dark or too bright, or the detected object is obscured by something else, the robot system equipped with only visual sensors is not able to complete the task. In this regard, it is necessary to develop alternative sensing technology. It is noted that a lot of research works are based on the imitation of biological systems, e.g., inspired by bats and birds, a robotic aircraft with flexible wings was modeled and controlled in [5]. Inspired by tactile sensing of humans, we aim to develop an approach of haptic identification for robots.

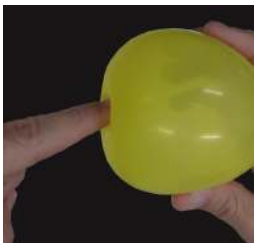

Fig. 1. Human interacting with an object using haptic exploration [photo taken at South China University of Technology]

It is heuristic that people identify the geometry and stiffness of various objects through the sense of touch (Fig. 1). Therefore, we may use specialized tactile sensors for robots to detect an object's properties, e.g., the intelligent haptic sensor based on force sensing resistor (FSR) could estimate an object's surface orientation [6]. However, most tactile sensors are delicate and require proper working conditions, which implies that appropriate tactile sensors need to be developed for specific robots. To make the estimation of the object's properties more feasible, we will develop a method without requiring any dedicated sensing hardware.

When humans interact with unknown external environments, we tend to adjust the force and impedance skillfully [7]. As studied in [8], when interacting with an unstable environment, the human central nervous system (CNS) tends to adjust the endpoint impedance of the limbs. It is indicated in [9] that humans tune the interaction force to counteract a compliant object, and adapt the reference trajectory around an external object during the interaction. According to the experiment results reported in [9], a computational model was

This work was partially supported by National Nature Science Foundation (NSFC) under Grants 61473120 and U1613223, Guangdong Provincial Natural Science Foundation 2014A030313266 and International Science and Technology Collaboration Grant 2015A050502017, Science and Technology Planning Project of Guangzhou 201607010006, and State Key Laboratory of Robotics and System (HIT) Grant SKLRS-2017-KF-05.

C. Yang, K. Huang, and C.-Y Su are with the Key Laboratory of Autonomous Systems and Networked Control, College of Automation Science and Engineering, South China University of Technology, Guangzhou, 510640 China. C.-Y. Su is on leave from Concordia University, Canada.

H. Cheng is with Center for Robotics, University of Electronic Science and Technology of China, 611731, Chengdu, Sichuan, China.

Y. Li is with Department of Bioengineering, Imperial College London, SW2 7AZ, UK.

built in [10] to online adjust the reference trajectory to match the observation in [9]. Similar to the above studies, a human-like learning controller in [11] recognized the elasticity and geometry of the interacting object by adapting the feedforward force and desired point, with an assumption that the robot manipulator model was invariant and known. However, usually the dynamic model of a robot is unknown and can be subject to uncertainties.

Generally, adaptive control does not need prior information of system parameters, making it proper to deal with systems with uncertainty. Adaptive learning impedance control without requirement of the prior knowledge of the robot manipulators was developed for physical robot-environment interaction in [12]. To deal with parameter uncertainties, adaptive technique was integrated into the cooperative control design for a hybrid partial differential equation-ordinary differential equation system in [13]. In [14], adaptive control based on Lyapunov's direct method was developed to deal with the uncertainties of the system parameters. In addition to the uncertainties, adaptive control is able to handle the nonlinearities in the system, e.g., a dynamic surface control method was integrated into an adaptive output feedback controller for the systems with uncertainties and nonlinearities [15]. Several updating laws were developed for estimation of the parameters of systems with nonlinearity [16]. Besides, various adaptive controllers were developed for tracking the reference path [17] [18]. A robust adaptive control method combined with fuzzy control was proposed in [19], with which the calculation burden was mitigated and the system became more robust. In [20], various adaptive designs were discussed and compared for the problem of aircraft auto-landing. In the above works, uncertainties in the system can be parameterized. When the system model is unknown or the uncertainties could not be parameterized, neural network (NN) can be employed for approximation.

Combining with other traditional controllers, NN control can be developed and applied into various fields, such as aircraft auto-landing [20], wind power generation [21] and robot manipulation. The NN approximation property is able to deal with systems with uncertainty and unknown dynamics [22] [23]. Thus, the approximation property has been widely applied in various fields. A NN based control design was developed to perform effective estimation of wind power generation, which might be influenced by wind velocity, wind orientation, air mass density and so on in [21]. To handle the problem of grasping an object by dual arms with uncertainties, NN was used to approximate both the uncertainties of the dual arms and the unknown nonlinearity of the manipulated object [24]. A NN based telerobot control strategy with graranteed performance was designed in [25]. The NN enhanced controller compensated for the unknown dynamics of both the manipulator and the external payload. In addition, NN can be used to compensate for the nonlinearity in the system dynamics and the input, e.g., NN was used to deal with the complex nonlinearity in the dynamics and stabilize the bus power system [26]. A NN enhanced constrained control allocation strategy was developed for overactuated aircrafts in [27], in which NN was used to handle the nonsymmetric input saturation constraint. Two RBF NNs were developed in [28] to compensate for the effect of input dead-zone and to approximate the unknown dynamics of the flexible manipulator. In practical applications, NN is always combined with other control methods to obtain a better performance. To compensate for the effects of uncertain dynamics and time-varying delays, the RBFNNs and wave variable approach were integrated into the teleoperation controller applied on a TouchX joystick [29]. An application of genetic algorithm (GA) based NN control on lithium-ion battery systems was studied in [30]. In the control design for an fault diagnosis system, the initialization and optimization of the connection weights of NN were handled by GA, which resulted in a lower error range. A commodity trading model mixing the NN and expert system was established in [31], which had advantages compared to rule-based and unaided NN approaches. In [32] [33], the control strategies based on both adaptive NN and disturbance observer were designed for large-scale systems and 3-DOF model helicopters with uncertainties, nonlinearities, and unknown external disturbance. A general projection NN was employed to handle the quadratic programming problem caused by model predictive control [34]. [35] developed an adaptive NN controller based on full-state feedback for an uncertain robot manipulator, which had full-state constraints. Besides, a radial basis function (RBF) NN enhanced controller was designed for robotic manipulators to perform a tracking task [36]. Moreover, NN was applied on controlling the discrete-time systems [37].

Although the NN control has extensive applications in many fields, it is limited by its inherent computational complexity. Extreme learning machine (ELM) is a unified framework of the generalized single-hidden layer feedforward networks (SLFN) [38] [39]. It is distinctive that the weights of input samples and the bias of activation functions can be randomly chosen in the training process of the ELM. In comparison with the traditional NN, the ELM has a number of advantages such as celerity of training speed, convenience for implementation, and minimal human intervention. The ELM has been frequently used in situations such as human face recognition [40], object classification, hypersonic flight and so on [41]. An online sequential learning algorithm (OS-ELM) for SLFNs with high rapidity and accuracy was developed in [42]. It is noteworthy that except the number of hidden nodes, no more parameters need to be selected. An improved ELM was proposed in [43] with a higher accuracy and a faster training speed than the traditional ELM. A real-time learning algorithm (RLA) was developed in [44], similar to the ELM with an ability to

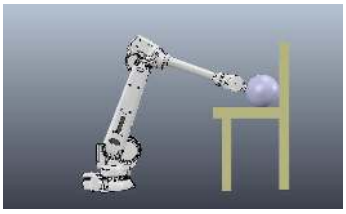

Fig. 2. An uncertain manipulator in contact with an unknown object

train massive samples accurately requiring a short time. A robust controller based on sliding-mode feedback control was developed in [45], which was able to improve the stability of the air graps in an electromagnetic actuated conveyance system.

In this work, we develop an ELM enabled adaptive learning control with finite-time convergence for uncertain manipulator to identify an object's geometry and elasticity, as shown in Fig. 2. First of all, due to the uncertainties of the robot manipulator dynamics, the ELM is employed to approximate the unknown manipulator's dynamic model. According to [46], to satisfy the persistent excitation (PE) condition, a periodic reference trajectory in the first trial is employed. In addition, we set a reference model whose feedforward force and reference point are updated iteratively, and the closed-loop robot system under the developed controller will match it exactly using the learned ELM weights in the first trail. Because the matching of the robot system to the reference model should be guaranteed before we update the model's reference point and feedforward force, we design learning law for the ELM to approximate the dynamic model in finite time.

Throughout this paper, the following notations are in order.

- $\|\cdot\|$ represents the induced norm of matrices and Euclidean norm of vectors.
- $[\ ]^T$ denotes the transpose of a vector or a matrix.
- $\mathbf{0}_{[p]}$ stands for a p-dimension zero vector.
- $I_{[m\times n]}$ represents a $m \times n$ unit matrix.

II. PRELIMINARIES

A. Kinematics and Dynamics

The kinematics of robot manipulator can be described as follows:

$$x(t) = \phi(q) \tag{1}$$

where $x(t) \in \mathbb{R}^n$ is the actual trajectory of the robot end-effector in the Cartesian space, $q \in \mathbb{R}^n$ represents the robot arm's joint position and n denotes the degree of freedom. Differentiating the forward kinematics with respect to time brings about the relationship between the task space velocity $\dot{x}$ and acceleration $\ddot{x}$ and the robot joint velocity $\dot{q}$ and joint acceleration $\ddot{q}$, respectively, i.e.,

$$\dot{x} = J(q)\dot{q},\ \ddot{x} = J(q)\ddot{q} + \dot{J}(q)\dot{q} \tag{2}$$

where $J(q) = \dfrac{\partial \phi}{\partial q} \in \mathbb{R}^{n\times n}$ denotes the relationship of velocities in the Cartesian space and joint space and it is called Jacobian matrix generally.

The dynamics of the robot manipulator is given by

$$M(q)\ddot{q} + C(q,\dot{q})\dot{q} + G(q) = \tau - J^T(q)f_I \tag{3}$$

where $M(q)$ is the inertia matrix, $G(q)$ is the torque of gravity, $C(q,\dot{q})$ represents the centrifugal and Coriolis matrix, τ is the control input in the joint space, and f_I is the external force from the interacting environment.

Because the recognition task is carried out in the Cartesian space, we perform transformation of the robot dynamics from the joint space to the Cartesion space. Integrating the kinematics (1)–(2) into the formulation (3), the dynamics of the robot in the task space can be described as below

$$M_x(q)\ddot{x} + C_x(q,\dot{q})\dot{x} + G_x(q) = \tau_x - f_I \tag{4}$$

where

$$\begin{aligned}
&M_x(q) = J^{-T}(q)M(q)J^{-1}(q),\\
&C_x(q,\dot{q}) = J^{-T}(q)(C(q,\dot{q}) - M(q)J^{-1}(q)\dot{J}(q))J^{-1}(q),\\
&G_x(q) = J^{-T}G(q),
\end{aligned}$$

$\tau_x = J^{-T}(q)\tau$, representing the control input which will be designed in this paper. The matrix $M_x(q)$ is symmetric positive definite. For the convenience, let us use the following abbreviation:

$$M_x = M_x(q),\ C_x = C_x(q,\dot{q}),\ G_x = G_x(q) \tag{5}$$

In accordance with [47], the following property will be used in the control design and performance analysis.

Property 1: The matrix $2C_x(q,\dot{q}) - \dot{M}_x(q)$ is skew symmetric.

B. Reference Model

The following desired reference model (Fig. 3) is defined to be followed by the actual manipulator as in [11]:

$$M_m\ddot{e} + C_m\dot{e} + K_m e = f_I - f_d \tag{6}$$

where $e = x_d - x$ with x_d the reference point in the task space, while f_d is the feedforward force for the robot maintaining a contact with the object, M_m and C_m are matrices denoting the desired mass, damping and K_m is the stiffness matrix. The selection of M_m, C_m and K_m depends on specific applications.

C. Control Objective

In this paper, we aim at designing a controller to make the manipulator dynamics follow the reference model (6). Meanwhile, by adjusting x_d and f_d iteratively, the manipulator

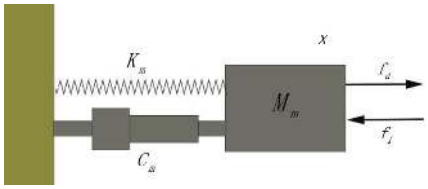

Fig. 3. The reference model represented by a mass-spring-damper system

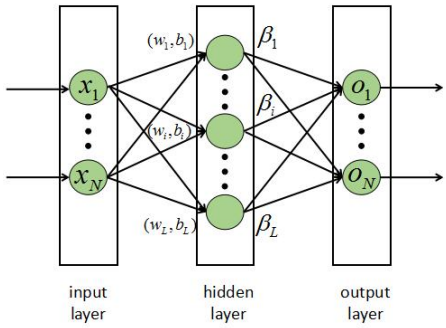

Fig. 4. The framework of the ELM

is able to detect the unknown object and estimate its stiffness and geometry (Fig.2). Define the matching error as follows

$$w = -M_m\ddot{e} - C_m\dot{e} - K_m e + f_I - f_d \tag{7}$$

Thus, the learning control strategy is to design a learning law ensuring the closed-loop system response to follow the specified reference model (6) in finite time. Equivalently, the matching error w will converge to zero in finite time, i.e.,

$$w = 0,\ t > t_c \tag{8}$$

where t_c is a terminating time. After ELM learning in the first trial, i.e., $w = 0$, the controlled system matches the reference model (6) without need of further learning. Thereafter, x_d and f_d in (6) will be updated from the second trial for haptic identification.

D. SLFN based on ELM

Considering a group of samples $(x_i, t_i), i = 1, 2, \cdots, N$ for training, and assuming that hidden nodes number is L, we see that a normal SLFN can be discribed as [48]

$$\sum_{i=1}^{L} \beta_i G(x_j; w_i, b_i) = o_j, j = 1, 2, \cdots, N \tag{9}$$

where w_i, b_i are the parameters linking the input samples with the hidden nodes, β_i represents the weight of hidden nodes in the neural output, and $G(x_j; w_i, b_i)$ represents the output of the ith hidden node depending on the input x_j. The framework of the ELM is shown in Fig. 4.

Let $\boldsymbol{x} = [x_1, x_2, \cdots, x_N], \boldsymbol{w} = [w_1, w_2, \cdots, w_L]$ and $\boldsymbol{b} = [b_1, b_2, \cdots, b_L]$. The standard SLFN described above is capable to approximate the samples accurately. Thus, we rewrite (9) as

$$\boldsymbol{H}(\boldsymbol{x}, \boldsymbol{w}, \boldsymbol{b})\beta = \boldsymbol{T} \tag{10}$$

in which

$$\boldsymbol{H}(x_1, x_2, \cdots, x_N, w_1, w_2, \cdots, w_L, b_1, b_2, \cdots, b_L)\beta = \begin{bmatrix} G(x_1, w_1, b_1) & \cdots & G(x_1, w_L, b_L) \\ \vdots & \ddots & \vdots \\ G(x_N, w_1, b_1) & \cdots & G(x_N, w_L, b_L) \end{bmatrix}$$

$$\beta = \begin{bmatrix} \beta_1 \\ \vdots \\ \beta_L \end{bmatrix}, T = \begin{bmatrix} t_1 \\ \vdots \\ t_N \end{bmatrix}$$

If we choose $L \leq N$, then the smallest norm least-squares solution of (10) can be obtained as

$$\hat{\beta} = \boldsymbol{H}^{\dagger}\boldsymbol{T} \tag{11}$$

where the matrix $\boldsymbol{H}^{\dagger}$ is the Moore-Penrose generalized inverse of $\boldsymbol{H}$.

III. Robotic Learning Control

In the following, let us design the learning control step by step. To facilitate the following design process, an alternative matching error is defined as

$$\bar{w} = K_f w = -\ddot{e} - K_d\dot{e} - K_p e + K_f(f_I - f_d) \tag{12}$$

where $K_d = M_m^{-1}C_m, K_p = M_m^{-1}K_m, K_f = M_m^{-1}$.

Let L represent Laplace transform operation and L^{-1} inverse Laplace transform operation. Define a filtered matching error z as below:

$$z = L^{-1}\{(1 - \frac{\Gamma}{s+\Gamma})L\{\dot{e}\} + \frac{1}{s+\Gamma}L\{\chi\}\} \tag{13}$$

where Γ is a positive constant scalar, and

$$\chi = -K_d\dot{e} - K_p e + K_f(f_I - f_d) \tag{14}$$

To simplify the calculation, we redesign the filtered matching error as

$$z = -\dot{e} + e_h + \chi_l = \begin{bmatrix} z_1 \\ z_2 \end{bmatrix} \tag{15}$$

where $e_h = L^{-1}\{\frac{\Gamma s}{s+\Gamma}L\{e\}\}$ represents the high-pass filtered signal, while $\chi_l = L^{-1}\{\frac{1}{s+\Gamma}L\{\chi\}\}$ denotes the low-pass filtered signal. Integrating (12)–(15), we can rewrite $\bar{w}$ as below

$$\bar{w} = \dot{z} + \Gamma z \tag{16}$$

It can be seen that $\dot{z} = 0$ and $z = 0$ will result in $w = 0$.

Define

$$M_x\ddot{x}_r + C_x\dot{x}_r + G_x = H(x, w, b)\beta^* + \epsilon(x) \tag{17}$$

where

$$\dot{x}_r = \dot{x}_d - e_h - \chi_l,\ \ddot{x}_r = \ddot{x}_d - \dot{e}_h - \dot{\chi}_l \tag{18}$$

β^* is the optimal parameter for the SLFN to approximate $M_x\ddot{x}_r + C_x\dot{x}_r + G_x$, and ϵ is the reconstruction error.

The control input is designed as

$$\tau_x = H\hat{\beta} - (S + K + K_\delta)\mathrm{sgn}(z) + \hat{f}_I \tag{19}$$

where $H\hat{\beta}$ is the ELM output torque, and $\hat{\beta}$ is the estimate of β^*; $S, K = \mathrm{diag}(k_1, k_2)$, and $K_\delta = \mathrm{diag}(k_{\delta 1}, k_{\delta 2})$ are all symmetric positive definite matrices, $k_{\delta 1}, k_{\delta 2} > \delta$, $\hat{f}_I$ is the measurement of external force f_I. $-K\mathrm{sgn}(z)$ is employed to compensate for the ELM approximation error. $-K_\delta\mathrm{sgn}(z)$ is used as a compensation of the measurement error. Besides, the measurement noise of force $\tilde{f}_I = \hat{f}_I - f_I \neq \mathbf{0}_{[n]}$ is bounded and the bound of the amplitude is known, i.e., $||\tilde{f}_I|| \leq \delta$.

Combining the input (19) with the robot dynamics in operational space (4), we obtain the following closed-loop dynamics

$$\begin{aligned} &M_x(q)\dot{z} + C_x(q,\dot{q})z + S\mathrm{sgn}(z) \\ =&(H\hat{\beta} - (M_x\ddot{x}_r + C_x\dot{x}_r + G_x)) \\ &-K\mathrm{sgn}(z) - (K_\delta\mathrm{sgn}(z) - \tilde{f}_I) \end{aligned} \tag{20}$$

Due to the requirement of updating x_d and f_d of the reference model in each trial, it is necessary to guarantee that the matching error w converges to zero in finite time.

By defining $X_r = [\ddot{x}_r; \dot{x}_r; I_{[n\times 1]}] \in \mathbb{R}^{3n\times 1}, X = [\ddot{x}; \dot{x}; I_{[n\times 1]}] \in \mathbb{R}^{3n\times 1}$ and combining (17), we have

$$\begin{aligned} M_x\ddot{x}_r + C_x\dot{x}_r + G_x &= [M_x, C_x, G_x]X_r \\ &= H\beta^* + \epsilon \end{aligned} \tag{21}$$

Thus, the robot dynamics can be represented as follows

$$\begin{aligned} M_x\ddot{x} + C_x\dot{x} + G_x &= [M_x, C_x, G_x]X \\ &= (H\beta^* + \epsilon)X_r^\dagger X \end{aligned} \tag{22}$$

where $X_r^\dagger \in \mathbb{R}^{1\times 3n}$ is the Moore-Penrose generalized inverse of vector X_r. Thus, $X_r^\dagger X$ is a scalar. (22) can be represented as

$$(H\beta^* + \epsilon)X_r^\dagger X = X_r^\dagger X(H\beta^* + \epsilon) = H_1\beta^* + \epsilon_1 \tag{23}$$

where $H_1 = X_r^\dagger XH$, and $\epsilon_1 = X_r^\dagger X\epsilon$. Therefore, the dynamics (4) can be represented as

$$H_1\beta^* + \epsilon_1 = \tau_1 - \tilde{f}_I \tag{24}$$

where $\tau_1 = H\hat{\beta} - (S + K + K_\delta)\mathrm{sgn}(z)$.

To derive the parameter learning law, let us define the filtered variables $H_f, \epsilon_f, \tau_f, f_f$ as

$$\begin{cases} l\dot{H}_f + H_f = H_1, H_f|_{t=0} = 0 \\ l\dot{\epsilon}_f + \epsilon_f = \epsilon_1, \epsilon_f|_{t=0} = 0 \\ l\dot{\tau}_f + \tau_f = \tau_1, \tau_f|_{t=0} = 0 \\ l\dot{\tilde{f}}_{If} + \tilde{f}_{If} = \tilde{f}_I, \tilde{f}_{If}|_{t=0} = 0 \end{cases} \tag{25}$$

where $l > 0$ is a filter parameter. Then, (24) can be rewritten as

$$H_f\beta^* = \tau_f - \tilde{f}_{If} - \epsilon_f \tag{26}$$

Define matrix $P \in \mathbb{R}^{N\times N}$ and vector $Q \in \mathbb{R}^N$ as

$$\begin{cases} \dot{P} = -\ell P + H_f^T H_f, P(0) = 0 \\ \dot{Q} = -\ell Q + H_f^T\tau_f, Q(0) = 0 \end{cases} \tag{27}$$

where ℓ is a design constant.

Let us consider an assistant vector $W \in \mathbb{R}^N$ depending on P, Q in (27) as

$$W = P\hat{\beta} - Q \tag{28}$$

Due to

$$\begin{aligned} Q &= \int_0^t e^{-\ell(t-r)}H_f^T(H_f\beta^* + \tilde{f}_{If} + \epsilon_f)dr \\ &= P\beta^* + \int_0^t e^{-\ell(t-r)}H_f^T(r)(\tilde{f}_{If}(r) + \epsilon_f(r))dr \end{aligned} \tag{29}$$

we obtain

$$W = -P\tilde{\beta} + \psi \tag{30}$$

where $\tilde{\beta} = \beta^* - \hat{\beta}$; $\psi = -\int_0^t e^{-\ell(t-r)}H_f^T(r)(\tilde{f}_{If}(r) + \epsilon_f(r))dr$ is bounded.

To guarantee the finite-time convergence of the estimation error $\tilde{\beta}$, we design the following learning law for $\hat{\beta}$ as in [16]:

$$\dot{\hat{\beta}} = -\Lambda\frac{P^TW}{\|W\|} \tag{31}$$

where Λ is a positive definite learning gain matrix.

From (30) we have $P^{-1}W = -\tilde{\beta} + P^{-1}\psi$. Differentiating $P^{-1}W$ with respect to time leads to

$$\frac{\partial(P^{-1}W)}{\partial t} = -\dot{\tilde{\beta}} + \frac{\partial P^{-1}}{\partial t}\psi + P^{-1}\dot{\psi} \tag{32}$$

In terms of $I = PP^{-1}$, differentiating PP^{-1} with respect to time, we have

$$\dot{P}P^{-1} + P\frac{\partial P^{-1}}{\partial t} = 0 \tag{33}$$

Thus, $\frac{\partial P^{-1}}{\partial t} = -P^{-1}\dot{P}P^{-1}$. Then, we have

$$\begin{aligned} \frac{\partial(P^{-1}W)}{\partial t} &= \dot{\hat{\beta}} - P^{-1}\dot{P}P^{-1}\psi + P^{-1}\dot{\psi} \\ &= \dot{\hat{\beta}} + \psi' \end{aligned} \tag{34}$$

where $\psi' = -P^{-1}\dot{P}P^{-1}\psi + P^{-1}\dot{\psi}$.

Select a Lyapunov function $V_1 = \frac{1}{2}W^TP^{-1}P^{-1}W$; then

$$\begin{aligned} \dot{V}_1 &= \frac{1}{2}\frac{\partial(W^TP^{-1})}{\partial t}P^{-1}W + \frac{1}{2}W^TP^{-1}\frac{\partial(P^{-1}W)}{\partial t} \\ &= W^TP^{-1}\frac{\partial(P^{-1}W)}{\partial t} \\ &= -W^TP^{-1}\Lambda\frac{P^TW}{\|W\|} + W^TP^{-1}\psi' \\ &\leq -(\lambda_{\min}(\Lambda) - \|P^{-1}\psi'\|)\|W\| \end{aligned} \tag{35}$$

Consider $\psi = -\int_0^t e^{-\ell(t-r)} H_f^T(r)(\tilde{f}_{If}(r) + \epsilon_f(r))dr$. It can be found that ψ and $\dot{\psi}$ are bounded as long as $\tilde{f}_I, \epsilon$ and $H_f(x)$ are bounded. The matrices P and $\dot{P}$ are also bounded for bounded $H_f(x)$. Moreover, according to [49], with a periodic or periodic-like input for the ELM, the matrix H is persistently excited (PE), i.e., there exist $T_1 > 0, \varrho > 0$ such that $\int_t^{t+T_1} H(r)H^T(r)dr \geq \varrho I, \forall t \geq 0$. According to (27) and Lemma 2.2 in [16], P is positive definite satisfying $\lambda_{\min}(P) > \sigma > 0$, where $\sigma = e^{-\ell T_1}\varrho$. It indicates the boundedness of P^{-1} in magnitude. Therefore, with an assumption of a bounded measurement noise of force $\tilde{f}_I$ and a bounded reconstruction error ϵ, $\|P^{-1}\psi'\|$ is bounded. Then, when Λ is large enough, i.e., $\lambda_{\min}(\Lambda) > \|P^{-1}\psi'\|$, W is readily bounded according to (35), and thus $\tilde{\beta}$ and $\hat{\beta}$ are also bounded.

To further analyze the error bound, we rewrite (35) as $\dot{V}_1 \leq -\mu_1\sqrt{V_1}$, where $\mu_1 = (\lambda_{\min}(\Lambda) - \|P^{-1}\psi'\|)\sigma\sqrt{2}$ is a positive scalar. When it is selected larger than a prespecified constant value, the convergence $\lim_{t\to t_a} V_1 = 0$ can be achieved. Thus, according to [50], the convergence of W can be ensured in a finite time $t_a \leq 2\sqrt{V(0)}/\mu_1$, i.e., $\lim_{t\to t_a} W = 0$, which leads to the convergence of estimation error $\lim_{t\to t_a} P\tilde{\beta} = \psi$.

The estimation error $\tilde{\beta}$ converges to a compact set in a finite time t_a which satisfies $\lim_{t\to t_a} P\tilde{\beta} = \psi$. Combining the closed-loop dynamics (20) with equation (21), we have

$$\begin{aligned} &M_x(q)\dot{z} + C_x(q,\dot{q})z + S\text{sgn}(z) \\ &= -(H\tilde{\beta} + \epsilon) - K\text{sgn}(z) - (K_\delta \text{sgn}(z) - \tilde{f}_I) \end{aligned} \tag{36}$$

Select a Lyapunov function $V_2 = \frac{1}{2}z^T M_x z$, then

$$\begin{aligned} \dot{V}_2 &= \frac{1}{2}\dot{z}^T M_x z + \frac{1}{2}z^T \dot{M}_x z + \frac{1}{2}z^T M_x \dot{z} \\ &= z^T M_x \dot{z} + \frac{1}{2}z^T \dot{M}_x z \\ &= z^T[-C_x z - S\text{sgn}(z) - (H\tilde{\beta} + \epsilon) - K\text{sgn}(z) \\ &\quad -(K_\delta \text{sgn}(z) - \tilde{f}_I)] + \frac{1}{2}z^T \dot{M}_x z \\ &= \frac{1}{2}z^T(\dot{M}_x - 2C_x)z - z^T S\text{sgn}(z) + z^T(-(HP^{-1}\psi + \epsilon) \\ &\quad -K\text{sgn}(z)) - z^T(K_\delta \text{sgn}(z) - \tilde{f}_I) \\ &= -z^T S\text{sgn}(z) + z^T(-(HP^{-1}\psi + \epsilon) - K\text{sgn}(z)) \\ &\quad -z^T(K_\delta \text{sgn}(z) - \tilde{f}_I) \end{aligned} \tag{37}$$

where we use the skew-symmetry property of $\dot{M}_x - 2C_x$ and the solution mentioned above that $\tilde{\beta} = P^{-1}\psi, t \geq t_a$. Denote $HP^{-1}\psi + \epsilon = \begin{bmatrix}(HP^{-1}\psi+\epsilon)_1 \\ (HP^{-1}\psi+\epsilon)_2\end{bmatrix}$. Because $HP^{-1}\psi$ and ϵ are bounded, thus, with the matrix $K = \text{diag}(k_1, k_2)$ properly chosen such that $k_1 \geq |(HP^{-1}\psi+\epsilon)_1|$ and $k_2 \geq |(HP^{-1}\psi+\epsilon)_2|$, we have

$$\begin{aligned} \dot{V}_2 &\leq -z^T S\text{sgn}(z) - |z_1|(k_1 - |(HP^{-1}\psi + \epsilon)_1|) - |z_2| \cdot \\ &\quad (k_2 - |(HP^{-1}\psi + \epsilon)_2|) - z^T(K_\delta \text{sgn}(z) - \tilde{f}_I) \\ &\leq -z^T S\text{sgn}(z) - z^T(K_\delta \text{sgn}(z) - \tilde{f}_I) \\ &\leq -z^T S\text{sgn}(z) \end{aligned} \tag{38}$$

where we use the fact $z^T(K_\delta \text{sgn}(z) - \tilde{f}_I) \geq 0$. Due to the boundedness of M_x, for a large enough S, we have $\dot{V}_2 \leq -\mu_2\sqrt{V_2}$, where μ_2 is a positive constant. According to [51], there exists a finite time t_b such that $\|z\| \equiv 0, \forall t > t_b$ after the finite time convergence of $\tilde{\beta}$. In a word, the filtered matching error z would converge to 0 in a finite time $t_c = t_a + t_b$, i.e., $\|z\| = 0, t \geq t_c$. In accordance with (12) and (16), the matching error $w = 0, t \geq t_c$.

From the above analysis, the parameter estimation error $\tilde{\beta}$ would converge to a compact set in a finite time t_a. The convergence of parameter estimation leads to the convergence of the matching error w in a finite time t_c, i.e., $w = 0, t \geq t_c$. Let the latter estimation $\hat{\beta}^k = \hat{\beta}^0(T)(k > 1)$, where $T > t_c$ is the period of the first trial which guarantees the matching error $w = 0$, and superscript "k" represents the kth trial to detect the external object. From the second trial, there is no need to re-learn the weight parameter $\hat{\beta}$ any more. Using the parameter estimation $\hat{\beta}$ learned in the first trial will guarantee that the matching error vanishes in a finite time t_b, i.e., from the second trial, there exists $w = 0, t > t_b$. Thereafter, x_d and f_d in the reference model will be updated iteratively to achieve the identification of the object's properties.

IV. Reference Model Adaptation

A. Adaptation of Reference Point and Feedforward Force

For ease of computation but without loss of generality, we assume that the robot manipulator detects the object only in one direction along the x axis of the operational space (Fig. 5). However, the control strategy can be applied on the three axes x, y and z in the same way. Suppose that the matrices C_m, K_m and initial reference point x_t are selected appropriately in each trial. Thus, the robot manipulator's movement and interaction with the unknown object are smooth and gentle without destroying the object. When the robot end-effector interacts with the object, we assume that the external force can be described as

$$f_I = K_0(x - x_b) \tag{39}$$

where K_0 represents the stiffness of the object and x_b the object's boundary.

In the first trial, the reference trajectory should be set to be periodic to satisfy the PE condition. From the second trial, for a better tracking performance, the reference point changes in a manner as in [52] as below

$$x_d(t) = x_d(0) + (x_d(T) - x_d(0))(10\bar{t}^3 - 15\bar{t}^4 + 6\bar{t}^5) \tag{40}$$

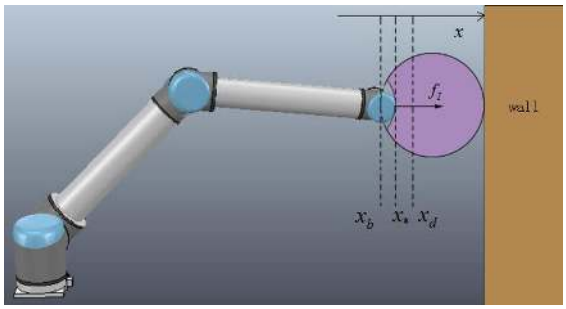

Fig. 5. Robot end-effector interacting with an unknown object on the wall and exploring its geometry and stiffness

where $\bar{t} \equiv \frac{2t}{T}$; and T is the movement duration. Let $x_d(T) = x_d^*$, where x_d^* is a constant in each trial which is the ultimate goal of the changing reference point x_d, and it will be adapted iteratively. On the other hand, $x_d(t)$ is the reference trajectory used by the robot in practice.

Combining (6) and (39), the closed-loop dynamics during interaction can be obtained as

$$M_m\ddot{e} + C_m\dot{e} + K_m e - K_0(x - x_b) = -f_d \tag{41}$$

Assume that a finite time t_f is taken by each trail, and it is sufficiently large so that at the end of each trial the interaction between the robot end-effector and the object has reached an equilibrium (the reference point x_d has reached the saturation x_d^* and never changes again). Consider the equilibrium position of the robot end-effector as x_*. From the above analysis, it can be seen that t_f should satisfy $t_f \geq t_c$. Since the error e no longer changes at the equilibrium point, its first derivative $\dot{e}$ and second derivative $\ddot{e}$ are equal to $\mathbf{0}_{[n]}$. Thus, the equilibrium point satisfies

$$K_0(x_* - x_b) = -K_m(x_* - x_d^*) + f_d \tag{42}$$

Denoting $v^k = x_*^k - x_d^k$, and according to [11], we use the adaptation law of reference point x_d and feedforward force f_d from one trial k to the next as follows

$$\begin{cases} x_d^{*1} = x_d^{*2} = x_t, \ k = 3, 4 \cdots \\ x_d^{*k+1} = x_d^{*k} + \alpha^k v^k + (1 - \alpha^k)(x_t - x_d^{*k}), \\ \qquad \text{if } v^k \leq 0 \\ x_d^{*k+1} = x_d^{*k} + (1 - \alpha^k)(x_t - x_d^{*k}), \ \text{otherwise} \end{cases} \tag{43}$$

$$\begin{cases} f_d^1 = f_d^2 = F_0, \ k = 3, 4, \cdots \\ f_d^{k+1} = f_d^k + K_m(v^k - v^{k-1}) + \zeta^k(F_0 - f_d^k), \\ \qquad \text{if } v^k \leq 0 \\ f_d^{k+1} = f_d^k + \zeta^k(F_0 - f_d^k), \ \text{otherwise} \end{cases} \tag{44}$$

where $0 < \alpha^k < 1$ is a factor that defines the compliance of the reference point to the object, while $0 < \zeta^k < 1$ represents a relaxing factor tending to maintain f_d to the default state F_0. They both will be designed latter.

B. Object Geometry and Elasticity Learning

According to [11], let us define

$$\begin{aligned} a_1 &\equiv \frac{K_m}{K_0}, \ a_2 \equiv x_b, \ s^k \equiv \frac{x_*^k}{x_*^k - x_d^{*k}} \\ \phi_1^k &\equiv \frac{f_d^k}{K_m(x_*^k - x_d^{*k})} - 1, \ \phi_2^k \equiv \frac{1}{x_*^k - x_d^{*k}} \end{aligned} \tag{45}$$

Combining (45) with the closed-loop dynamics (20), we obtain

$$A^T\Phi^k = s^k \tag{46}$$

where $A = [a_1, a_2]^T$ and $\Phi = [\phi_1, \phi_2]^T$.

Due to the linearity of parameters in (46), a weighted least square (WLS) [53] can be employed for fast convergence as below

$$\begin{aligned} \hat{A}^{k+1} &= \hat{A}^k + L^k(s^{k+1} - (\hat{A}^k)^T\Phi^k) \\ L^k &= \frac{P^k\Phi^k}{d^{k^{-1}} + (\Phi^k)^T P^k \Phi^k} \\ P^{k+1} &= P^k - \frac{P^k\Phi^k(\Phi^k)^T P^k}{\sigma^{k^{-1}} + (\Phi^k)^T P^k \Phi^k} \end{aligned} \tag{47}$$

where $k = 3, 4, \cdots$, and $\hat{A}^k = [\hat{a}_1^k, \hat{a}_2^k]^T$ with $\hat{a}_1^k$ and $\hat{a}_2^k$ the estimates of a_1 and a_2, respectively. Then, the estimates of K_0 and x_b at the kth trial are represented as $\hat{K}_0^k$ and $\hat{x}_0^k$, respectively, which are obtained by

$$\hat{K}_0^k \equiv \frac{K_m}{\hat{a}_1^k}, \ \hat{x}_b^k \equiv \hat{a}_2^k, \ \text{if } v^k \leq 0 \tag{48}$$

Theoretically, the initial value of $\hat{A}$, i.e., $\hat{A}^1$, can be selected arbitrarily. Practically, the initial estimates of x_b and K_0 are chosen as $\hat{x}_b = x_s$ and $\hat{K}_0^2 = \hat{K}_0^1 = \bar{K}_0$, where x_s and $\bar{K}_0$ are the initial position of end-effector and the largest possible stiffness of the detected object, respectively. This is because when we humans explore the environment by hand without vision, we prefer to assume the unknown object hard and large. When $v^k > 0$, it can be assumed that the object has been moved away or replaced by another object (if neither occurs but just an extra feedforward force, the adaptation law (44) will reduce f_d such that v^k will be nonpositive again), so according to [11], we have

$$\hat{K}_0^k \equiv \zeta^k\hat{K}_0^{k-1}, \hat{x}_b^k \equiv \alpha^k\hat{x}_b^{k-1} + (1 - \alpha^k)x_t, \ \text{if } v^k > 0 \tag{49}$$

In addition, P in (47) can be initialized as an identity matrix, e.g., $P^1 = I$. The weighting sequence d^k can be obtained by

$$d^k = \frac{1}{\log^{1+\gamma}(1 + \sum_{i=0}^k \|\Phi^i\|^2)} \tag{50}$$

where γ is a positive constant. With $\hat{K}_0$ available, we can acquire the compliance factor α^k and the relaxing factor ζ^k in (43) (44) as

$$\alpha^k = \lambda\frac{\hat{K}_0}{\bar{K}_0}, \ \zeta^k = 1 - \alpha^k \tag{51}$$

where λ is a constant specified by the designer.

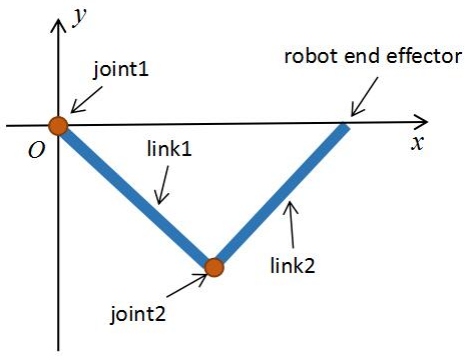

Fig. 6. A 2-degrees-of-freedom robot model

V. SIMULAION STUDIES

To test the validity of our proposed identification method, we carry out simulation studies on a robot manipulator which moves in the $x-y$ plane as shown in Fig. 6. There will be two scenarios with case (i) interacting with a spring, and case (ii) interacting with three circular objects with different radius and stiffness, respectively.

In the following, m_i and l_i are the mass and the length of the link i, l_{ci} is the distance between the $(i-1)$th joint and the ith link's mass center, $i=1,2$. I_i is the moment inertia of link i. According to [12], we set $m_1=m_2=10.0kg, l_1=l_2=1.0m, I_1=I_2=0.83kgm^2, l_{c1}=I_{c2}=0.5m$. Let us use the following abbreviation:

$$\begin{aligned} &s_{12}=\sin(q_1+q_2), c_{12}=\cos(q_1+q_2),\\ &s_1=\sin(q_1), s_2=\sin(q_2),\\ &c_1=\cos(q_1), c_2=\cos(q_2) \end{aligned} \tag{52}$$

Then, the kinematic constraints in (2) and the dynamics (3) are given by

$$J(q)=\begin{bmatrix} -(l_1s_1+l_2s_{12}) & -l_2s_{12} \\ l_1c_1+l_2c_{12} & l_2c_{12} \end{bmatrix} \tag{53}$$

$$J^{-1}(q)=\frac{1}{l_1l_2s_2}\begin{bmatrix} l_2c_{12} & l_2s_{12} \\ -(l_1c_1+l_2c_{12}) & -(l_1s_1+l_2s_{12}) \end{bmatrix} \tag{54}$$

and

$$\begin{aligned} &M(q)=\begin{bmatrix} M_{11} & M_{12} \\ M_{21} & M_{22} \end{bmatrix},\ C(q,\dot{q})=\begin{bmatrix} C_{11} & C_{12} \\ C_{21} & C_{22} \end{bmatrix},\\ &G(q)=0 \end{aligned} \tag{55}$$

where

$$\begin{aligned} &M_{11}=m_1l_{c1}^2+m_2(l_1^2+l_{c2}^2+2l_1l_{c2}c_2)+I_1+I_2,\\ &M_{12}=M_{21}=m_2(l_{c2}^2+l_1l_{c2}c_2)+I_2,\\ &M_{22}=m_2l_{c2}^2+I_2,\ C_{11}=-m_2l_1l_{c2}s_2\dot{q}_2,\\ &C_{12}=-m_2l_1l_{c2}s_2(\dot{q}_1+\dot{q}_2),\\ &C_{21}=m_2l_1l_{c2}s_2\dot{q}_1,\ C_{22}=0 \end{aligned} \tag{56}$$

The robot end-effector positions in the operational space are initialized as

$$x^k(0)=1.0m, y^k(0)=0m \tag{57}$$

In the first trial, to satisfy the PE condition, the periodic reference trajectory is set as

$$x_d^0(t)=1+|\sin(\frac{\pi}{5}t)|,\ y_d^0(t)=0 \tag{58}$$

where $t\in[0,T]$. From the second trial, the reference trajectory is set as in (40). In the first simulation for parameter estimation, $T=30s>t_c$, which guarantees the convergence of the parameter estimation. From the next trial, $T=10s$ which is enough to make the matching error $w=0$ and the robot manipulator reach the equilibrium point x_*.

The object applies an external force to the robot end-effector in the manner as follows

$$f_I^k=\begin{cases} 0,\ x^k<x_b; \\ K_0(x^k-x_b), x^k\geq x_b. \end{cases} \tag{59}$$

where K_0 and x_b are the elasticity and boundary of the detected object. The error occurring in the force measurement $\tilde{f}_d$ is considered to be random and its amplitude is not greater than 1.

The parameters in reference model (6) are set as

$$M_m=10I_{[2\times2]},\ C_m=80I_{[2\times2]},\ G_m=15I_{[2\times2]} \tag{60}$$

The control parameters in (19) and learning gain in (31) are chosen as

$$\begin{aligned} &S=10I_{[2\times2]}, K=3I_{[2\times2]}, K_\delta=2I_{[2\times2]},\\ &l=0.005, \Gamma=1, \ell=50, \Lambda=0.1 \end{aligned} \tag{61}$$

The number of hidden neurons is 20, and the hidden neurons parameters w,b are set randomly in the intervals $[-1,1]$ and $[0,1]$, respectively.

The initial feedforward force is chosen as $F_0=0N$. The largest possible stiffness of object is selected as $\bar{K}_0=200N/m$.

A. Interaction with a spring

Consider that the spring exerts an external force against the manipulator only along the x axis, and its elasticity and rest position are $50N/m$ and $1.3m$, respectively. Using the periodic reference trajectory as in (58), the estimated parameter $\hat{\beta}^0$ and the matching error w^0 in the first trial are shown in Figs. 8 and 9, respectively. It can be seen that at the end of the first trial the ELM enhanced controller can obtain an estimated output weight vector $\hat{\beta}^0$ stably which guarantees the system matching the reference model with a small error in finite time. Then in the next trial, we just let $\hat{\beta}^k=\hat{\beta}^0(T), k\geq1$ which guarantees that the matching error w converges to zero.

Then, from the second trial, we update the reference point x_d^* and feedforward force f_d in the reference model iteratively

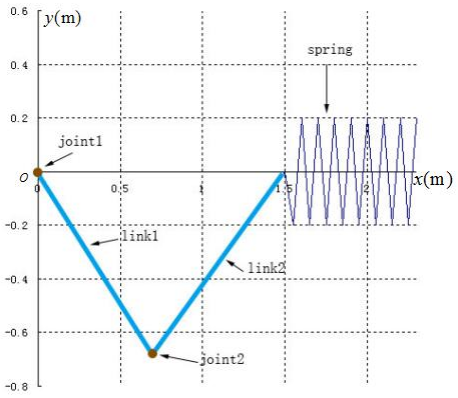

Fig. 7. A robot manipulator in contact with a spring (top view)

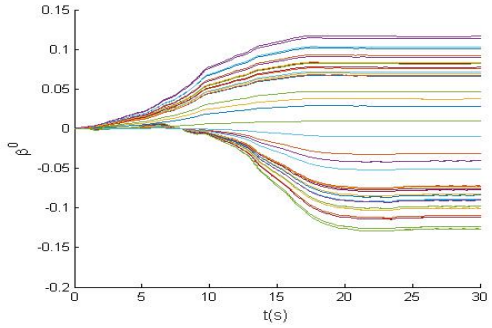

Fig. 8. The estimated parameter $\hat{\beta}^0$ in the first trial

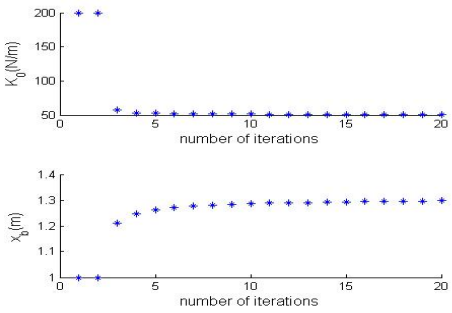

Fig. 10. The estimation of the spring's elasticity K_0 and rest position x_b when $K_0 = 50N/m, x_b = 1.3m$

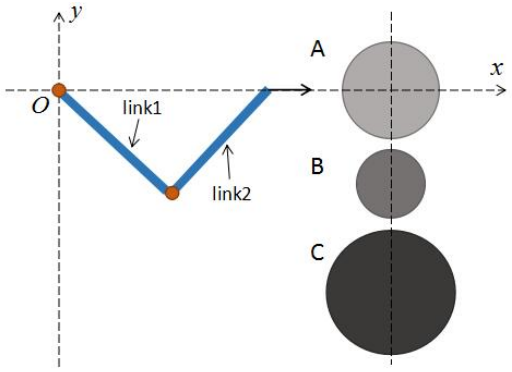

Fig. 11. Robot in interaction with three circular objects respectively

according to the adaptation laws (39) and (40). We set 20 trials for exploration, and the estimations of K_0 and x_b of the spring are shown in Fig. 10. The result shows that with the learned output weight vector of the ELM compensating for the nonlinear dynamics, the robot manipulator can estimate the stiffness and the rest position of the spring exactly.

B. Interaction with circular objects

The setup of the robot manipulator interacting with circular objects is illustrated in Fig. 11, in which the robot end-effector moves and approaches the object in the x direction from left to right. The three circular objects A, B and C with different radius and elasticities will be put in the specified locations in turn to be detected by the robot. Their centers are at $(1.6, 0)$, and the diameter and the elasticity of the three objects are $0.4m$ and $50N/m$; $0.6m$ and $70N/m$; $0.3m$ and $100N/m$, respectively.

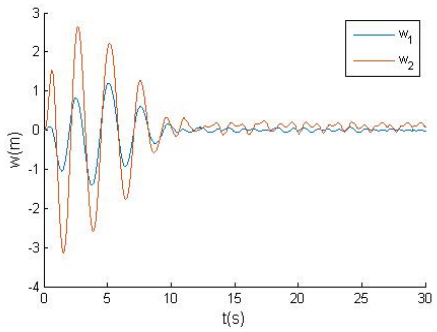

Fig. 9. The matching error w^0 in the first trial

The matching error w in the first trial when the robot detects each circular object, and the estimation of their elasticity K_0 and boundary x_b are illustrated in Figs. 12-17. Figs. 12,14,16 illustrate that although the initial values of the hidden neurons parameters w, b are set randomly, the proposed ELM enhanced controller could always compensate for the nonlinearity of the robot dynamics and approach the reference model in finite time with a small matching error. The simulation results imply that using our ELM enhanced controller, the robot with uncertainty can estimate the unknown object's stiffness and boundary successfully.

VI. Conclusion

This paper develops an ELM enhanced controller for uncertain robot manipulators to perform haptic identification. The ELM is used to compensate for the unknown non-linearity in the closed-loop dynamics. Eventually, the ELM enhanced

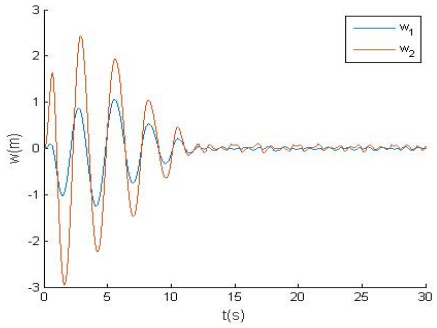

Fig. 12. The matching error w^0 in the first trial when the robot detects the object A

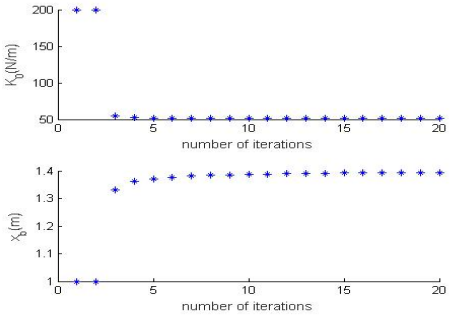

Fig. 13. The estimation of the object A's elasticity K_0 and rest position x_b when $K_0 = 50N/m, x_b = 1.4m$

controller ensures that the closed-loop dynamics follows a specified reference model, in which the feedforward force and reference point are adjusted iteratively for identification of elasticity and geometry of the detected object. In addition, the neural weight learning laws of the ELM are specially designed to guarantee the finite-time convergence of the learning errors of neural weights. As a result, the exact matching of the reference model can be achieved after the first iteration. Extensive simulations have been carried out to examine and demonstrate the validity and effectiveness of our control design.

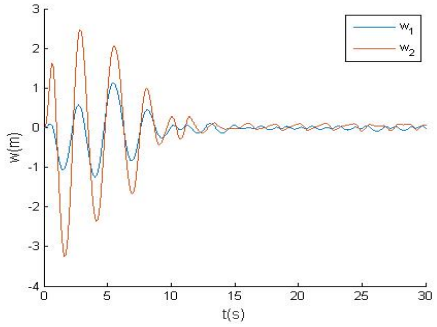

Fig. 14. The matching error w^0 in the first trial when the robot detects the object B

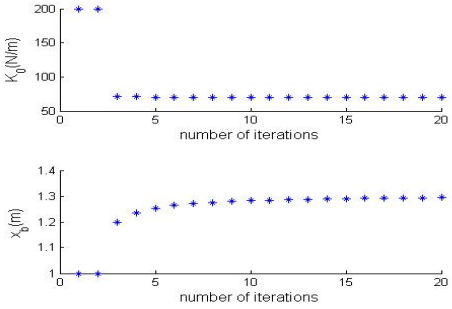

Fig. 15. The estimation of the object B's elasticity K_0 and rest position x_b when $K_0 = 70N/m, x_b = 1.3m$

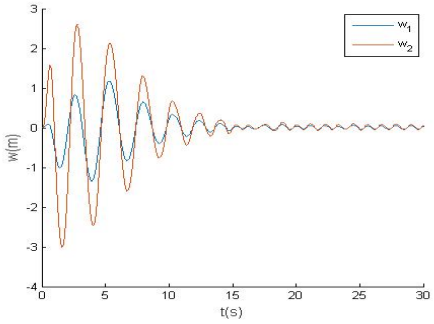

Fig. 16. The matching error w^0 in the first trial when the robot detects the object C

REFERENCES

[1] J. Luh, "An anatomy of industrial robots and their controls," *IEEE Transactions on Automatic Control*, vol. 28, no. 2, pp. 133–153, 1983.

[2] D. Nakhaeinia, S. H. Tang, S. B. M. Noor, and O. Motlagh, "A review of control architectures for autonomous navigation of mobile robots," *International Journal of Physical Sciences*, vol. 6, no. 2, pp. 169–174, 2011.

[3] A. K. Forrest, "Robot vision," *Physics in Technology*, vol. 17, no. 17, pp. 5–9, 1986.

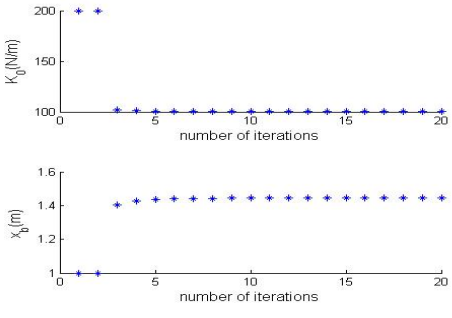

Fig. 17. The estimation of the object C's elasticity K_0 and rest position x_b when $K_0 = 100N/m, x_b = 1.45m$

[4] Y. Hu, Z. Li, G. Li, and P. Yuan, "Development of sensory-motor fusion-based manipulation and grasping control for a robotic hand-eye system," *IEEE Transactions on Systems Man & Cybernetics: Systems*, in press, DOI: 10.1109/TSMC.2016.2560530.

[5] W. He and S. Zhang, "Control design for nonlinear flexible wings of a robotic aircraft," *IEEE Transactions on Control Systems Technology*, vol. 25, no. 1, pp. 351–357, 2017.

[6] P. Payeur, C. Pasca, A. M. Cretu, and E. M. Petriu, "Intelligent haptic sensor system for robotic manipulation," *IEEE Transactions on Instrumentation & Measurement*, vol. 54, no. 4, pp. 1583–1592, 2005.

[7] E. Burdet, R. Osu, D. W. Franklin, T. E. Milner, and M. Kawato, "The central nervous system stabilizes unstable dynamics by learning optimal impedance," *Nature*, vol. 414, no. 6862, pp. 446–449, 2001.

[8] D. W. Franklin, G. Liaw, T. E. Milner, R. Osu, E. Burdet, and M. Kawato, "Endpoint stiffness of the arm is directionally tuned to instability in the environment," *Journal of Neuroscience*, vol. 27, no. 29, pp. 7705–7716, 2007.

[9] V. S. Chib, J. L. Patton, K. M. Lynch, and F. A. Mussa-Ivaldi, "Haptic identification of surfaces as fields of force," *Journal of Neurophysiology*, vol. 95, no. 2, pp. 1068–1077, 2006.

[10] C. Yang and E. Burdet, "A model of reference trajectory adaptation for interaction with objects of arbitrary shape and impedance," in *Proceedings of IEEE/RSJ International Conference on Intelligent Robots and Systems*, pp. 4121–4126, 2011.

[11] C. Yang, Z. Li, and E. Burdet, "Human like learning algorithm for simultaneous force control and haptic identification," in *Proceedings of IEEE/RSJ International Conference on Intelligent Robots and Systems*, pp. 710–715, 2013.

[12] Y. Li, S. Sam Ge, and C. Yang, "Learning impedance control for physical robotcenvironment interaction," *International Journal of Control*, vol. 85, no. 2, pp. 182–193, 2012.

[13] W. He and S. S. Ge, "Cooperative control of a nonuniform gantry crane with constrained tension," *Automatica*, vol. 66, no. C, pp. 146–154, 2016.

[14] W. He, S. Zhang, and S. S. Ge, "Robust adaptive control of a thruster assisted position mooring system," *Automatica*, vol. 50, no. 7, pp. 1843–1851, 2014.

[15] Y. J. Liu and W. Wang, "Adaptive output feedback control of uncertain nonlinear systems based on dynamic surface control technique," *International Journal of Robust and Nonlinear Control*, vol. 22, no. 9, pp. 945–958, 2012.

[16] J. Na, M. N. Mahyuddin, G. Herrmann, X. Ren, and P. Barber, "Robust adaptive finite-time parameter estimation and control for robotic systems," *International Journal of Robust and Nonlinear Control*, vol. 25, no. 16, pp. 3045–3071, 2014.

[17] P. A. Ioannou and J. Sun, *Robust Adaptive Control*. Prentice-Hall, Inc., 1984.

[18] S. Sastry, M. Bodson, and J. F. Bartram, "Adaptive control: Stability, convergence, and robustness," *Journal of the Acoustical Society of America*, vol. 88, no. 1, pp. 588–589, 1990.

[19] Y. J. Liu, W. Wang, S. C. Tong, and Y. S. Liu, "Robust adaptive tracking control for nonlinear systems based on bounds of fuzzy approximation parameters," *IEEE Transactions on Systems Man & Cybernetics: Systems*, vol. 40, no. 1, pp. 170–184, 2010.

[20] D. V. Prokhorov, R. A. Santiago, and D. C. W. Ii, "Adaptive critic designs: A case study for neurocontrol," *Neural Networks*, vol. 8, no. 9, pp. 1367–1372, 1995.

[21] S. Li, "Using neural network to estimate wind turbine power generation," *IEEE Transactions on Energy Conversion*, vol. 16, no. 3, pp. 276–282, 2001.

[22] Y. Jiang, C. Yang, S. L. Dai, and B. Ren, "Deterministic learning enhanced neutral network control of unmanned helicopter," *International Journal of Advanced Robotic Systems*, in press, DOI: 10.1177/1729881416671118.

[23] C. Sun, W. He, W. Ge, and C. Chang, "Adaptive neural network control of biped robots," *IEEE Transactions on Systems Man & Cybernetics: Systems*, vol. 47, no. 2, pp. 315–326, 2017.

[24] C. Yang, Y. Jiang, Z. Li, W. He, and C. Y. Su, "Neural control of bimanual robots with guaranteed global stability and motion precision," *IEEE Transactions on Industrial Informatics*, in press, 2016, DOI: 10.1109/TII.2016.2612646.

[25] C. Yang, X. Wang, L. Cheng, and H. Ma, "Neural-learning-based telerobot control with guaranteed performance," *IEEE Transactions on Cybernetics*, in press, 2016, DOI: 10.1109/TCYB.2016.2573837.

[26] W. Liu, G. K. Venayagamoorthy, J. Sarangapani, D. C. Wunsch, M. L. Crow, L. Liu, and D. A. Cartes, "Comparisons of an adaptive neural network based controller and an optimized conventional power system stabilizer," in *Proceedings of the IEEE International Conference on Control Applications*, pp. 922–927, 2007.

[27] M. Chen, "Constrained control allocation for overactuated aircraft using a neurodynamic model," *IEEE Transactions on Systems Man & Cybernetics: Systems*, vol. 46, no. 12, pp. 1630–1641, 2016.

[28] W. He, Y. Ouyang, and J. Hong, "Vibration control of a flexible robotic manipulator in the presence of input deadzone," *IEEE Transactions on Industrial Informatics*, vol. 13, no. 1, pp. 48–59, 2017.

[29] C. Yang, X. Wang, Z. Li, Y. Li, and C. Y. Su, "Teleoperation control based on combination of wave variable and neural networks," *IEEE Transactions on Systems Man & Cybernetics: Systems*, in press, 2016, DOI: 10.1109/TSMC.2016.2615061.

[30] Z. Gao, S. C. Cheng, W. L. Woo, and J. Jia, "Genetic algorithm based back-propagation neural network approach for fault diagnosis in lithium-ion battery system," in *Proceedings of the International Conference on Power Electronics Systems and Applications*, pp. 1–6, 2015.

[31] K. Bergerson and I. Wunsch, Donald C., "A commodity trading model based on a neural network-expert system hybrid," in *IJCNN-91-Seattle International Joint Conference on Neural Networks*, pp. 289–293, 1991.

[32] M. Chen and G. Tao, "Adaptive fault-tolerant control of uncertain nonlinear large-scale systems with unknown dead zone," *IEEE Transactions on Cybernetics*, vol. 46, no. 8, pp. 1851–1862, 2015.

[33] M. Chen, P. Shi, and C. Lim, "Adaptive neural fault-tolerant control of a 3-dof model helicopter system," *IEEE Transactions on Systems Man & Cybernetics: Systems*, vol. 46, no. 2, pp. 260–270, 2016.

[34] Z. Li, H. Xiao, C. Yang, and Y. Zhao, "Model predictive control of nonholonomic chained systems using general projection neural networks optimization," *IEEE Transactions on Systems Man & Cybernetics Systems*, vol. 45, no. 10, pp. 1313–1321, 2015.

[35] W. He, Y. Chen, and Z. Yin, "Adaptive neural network control of an uncertain robot with full-state constraints," *IEEE Transactions on Cybernetics*, vol. 46, no. 3, pp. 620–629, 2016.

[36] W. He, Y. Dong, and C. Sun, "Adaptive neural impedance control of a robotic manipulator with input saturation," *IEEE Transactions on Systems Man & Cybernetics: Systems*, vol. 46, no. 3, pp. 334–344, 2016.

[37] Y. Jiang, C. Yang, and H. Ma, "A review of fuzzy logic and neural network based intelligent control design for discrete-time systems," *Discrete Dynamics in Nature and Society*, vol. 2016, no. 4, pp. 1–11, 2016.

[38] G. B. Huang, Q. Y. Zhu, and C. K. Siew, "Extreme learning machine: Theory and applications," *Neurocomputing*, vol. 70, no. 1-3, pp. 489–501, 2006.

[39] C. W. Deng, G. B. Huang, J. Xu, and J. X. Tang, "Extreme learning machines: new trends and applications," *Science China Information Sciences*, vol. 58, no. 2, pp. 1–16, 2015.

[40] A. A. Mohammed, R. Minhas, Q. M. J. Wu, and M. A. Sid-Ahmed, "Human face recognition based on multidimensional pca and extreme learning machine," *Pattern Recognition*, vol. 44, no. 10-11, pp. 2588–2597, 2011.

[41] R. Minhas, A. A. Mohammed, and Q. M. J. Wu, "A fast recognition framework based on extreme learning machine using hybrid object information," *Neurocomputing*, vol. 73, no. 10-12, pp. 1831–1839, 2010.

[42] N. Y. Liang, G. B. Huang, P. Saratchandran, and N. Sundararajan, "A fast and accurate online sequential learning algorithm for feedforward networks," *IEEE Transactions on Neural Networks*, vol. 17, no. 6, pp. 1411–1423, 2006.

[43] H. S. Ke and X. L. Huang, "An improved extreme learning machine," in *Proceedings of the 32nd Chinese Control Conference*, pp. 3232–3237, 2013.

[44] G. B. Huang, Q. Y. Zhu, and C. K. Siew, "Real-time learning capability of neural networks," *IEEE Transactions on Neural Networks*, vol. 17, no. 4, pp. 863–878, 2006.

[45] C. S. Chin and C. Wheeler, "Sliding-mode control of an electromagnetic actuated conveyance system using contactless sensing," *IEEE Transactions on Industrial Electronics*, vol. 60, no. 11, pp. 5315–5324, 2013.
[46] S. L. Dai, C. Wang, and M. Wang, "Dynamic learning from adaptive neural network control of a class of nonaffine nonlinear systems," *IEEE Transactions on Neural Networks & Learning Systems*, vol. 25, no. 1, pp. 111–123, 2014.
[47] C. Yang, H. Ma, and M. Fu, *Advanced Technologies in Modern Robotic Applications*. Springer Singapore, 2016.
[48] R. Cui, C. Yang, Y. Li, and S. Sharma, "Adaptive neural network control of auvs with control input nonlinearities using reinforcement learning," *IEEE Transactions on Systems, Man, & Cybernetics: Systems*, in press, 2017, DOI: 10.1109/TSMC.2016.2645699.
[49] S. L. Dai, M. Wang, and C. Wang, "Neural learning control of marine surface vessels with guaranteed transient tracking performance," *IEEE Transactions on Industrial Electronics*, vol. 63, no. 3, pp. 1717–1727, 2015.
[50] V. I. Utkin, *Sliding Modes in Control and Optimization*. Springer-Verlag, 1992.
[51] C. Yang, Z. Li, R. Cui, and B. Xu, "Neural network-based motion control of an underactuated wheeled inverted pendulum model," *IEEE Transactions on Neural Networks & Learning Systems*, vol. 25, no. 11, pp. 2004–2016, 2014.
[52] A. M. C. Smith, C. Yang, H. Ma, P. Culverhouse, A. Cangelosi, and E. Burdet, "Novel hybrid adaptive controller for manipulation in complex perturbation environments," *Plos One*, vol. 10, no. 6, p. e0129281, 2015.
[53] L. Guo, "Self-convergence of weighted least-squares with applications to stochastic adaptive control," *IEEE Transactions on Automatic Control*, vol. 41, no. 1, pp. 79–89, 1996.

Chenguang Yang (M'10-SM'16) received the B.Eng. degree in measurement and control from Northwestern Polytechnical University, Xi'an, China, in 2005, and the Ph.D. degree in control engineering from the National University of Singapore, Singapore, in 2010. He received postdoctoral training at Imperial College London, UK. He is with Zienkiewicz Centre for Computational Engineering, Swansea University, UK, as a senior lecturer and is also with South China Univeristy of Technology, China. His research interests lie in robotics, automation and computational intelligence.

Kunxia Huang received the B.E. degree in automation from South China University of Technology, Guangzhou, China, in 2016, and is currently working toward the M.S. degree at the South China University of Technology, Guangzhou, China. Her research interests include robotics and robot haptic identification.

Hong Cheng (M'06-SM'14) Dr. Hong Cheng is professor of School of Automation Engineering and deputy director of Center for Robotics, Machine Intelligence Institute, University of Electronic Science and Technology of China, Chengdu, China from 2010. His research interests include machine learning and pattern recognition, computer vision and robotics. He has hosted and completed 5 NSFC general projects and major projects, and several enterprise horizontal projects. His achievements including exoskeleton and intelligent vehicle produced large social and economic benefits. In 2004, he hosted and finished the pilotless automobile SpringRobot of Xian Jiaotong University. And the exoskeleton system AIDER has been successfully developed in 2015. AIDER was worn by a disabled torch bearer on The Ninth Paralympic Games of China. The first production of AIDER system was published in 2016. In academic area, Prof. Cheng has published 3 monographs and teaching materials. He also has 100 papers published on top international magazines and conferences, which were quoted 1100 times on google scholar and H-factor was 16. In addition, 80 patents were applied for by Prof. Cheng. Dr. Cheng is the recipient of the New Century Talents Scheme of China in 2010 by MOE, and selected as Thousand Talents Program of Sichuan Province in 2013. He is a senior member of IEEE and served as a chief editor of IEEE Computational Intelligence Magazine from 2008 to 2010. And he also took charge of a financial chair of IEEE International Conference of Multimedia and Expo (ICME) 2014, a general chair of Vision and Learning Seminar (VALSE) 2015, a financial chair of China Summit & International Conference on Signal and Information Processing (ChinaSIP) 2015, a program chair of Chinese Conference on Pattern Recognition (CCPR) 2016, a general chair of China Conference on Social Robotics (CCSR) 2016 and an editor of special issue on Mechatronics Design and Control Strategies for Compliant Robotics of Assembly Automation.

Yanan Li (S'10-M'14) received the BEng and MEng degrees from the Harbin Institute of Technology, China, in 2006 and 2008, respectively, and the Ph.D. degree from the NUS Graduate School for Integrative Sciences and Engineering, National University of Singapore, in 2013. He has been a Research Scientist with the I2R, A*STAR, from 2013 to 2015. He is currently a Research Associate with the Department of Bioengineering, Imperial College London, UK. His research interests include physical human-robot interaction and robot control.

Chun-Yi Su (SM'99) received the Ph.D. degree in control engineering from the South China University of Technology, Guangzhou, China, in 1990. He joined Concordia University, Montreal, QC, Canada, in 1998, after a seven-year stint with the University of Victoria, Victoria, BC, Canada. He is currently with the College of Automation Science and Engineering, South China University of Technology, on leave from Concordia University. His current research interests include the application of automatic control theory to mechanical systems. He is particularly interested in control of systems involving hysteresis nonlinearities. He has authored or co-authored over 300 publications in journals, book chapters, and conference proceedings. Dr. Su has served as an Associate Editor of the IEEE TRANSACTIONS ON AUTOMATIC CONTROL, the IEEE TRANSACTIONS ON CONTROL SYSTEMS TECHNOLOGY, and the Journal of Control Theory and Applications. He has been on the Editorial Board of 18 journals, including the IFAC Journal of Control Engineering Practice and Mechatronics.